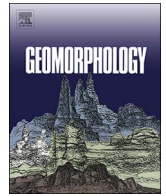




ELSEVIER

Contents lists available at ScienceDirect

Geomorphology

journal homepage: www.elsevier.com/locate/geomorph

Stepwise morphological evolution of the active Yellow River (Huanghe) delta lobe (1976–2013): Dominant roles of riverine discharge and sediment grain size

Xiao Wu^{a,b}, Naishuang Bi^{a,b}, Jingping Xu^{a,b}, Jeffrey A. Nittrouer^c, Zuosheng Yang^{a,b},
Yoshiki Saito^{d,e}, Houjie Wang^{a,b,*}

^a College of Marine Geosciences, Key Laboratory of Submarine Geosciences and Prospecting Technology, Ocean University of China, 238 Songling Road, Qingdao 266100, PR China

^b Laboratory for Marine Geology, Qingdao National Laboratory for Marine Science and Technology (QNLMT), Qingdao 266061, China

^c Department of Earth Science, Rice University, Houston, TX 77251, USA

^d Geological Survey of Japan (GSJ), National Institute of Advanced Industrial Science and Technology (AIST), Central 7, Higashi 1-1-1, Tsukuba, Ibaraki 305-8567, Japan

^e Research Center for Coastal Lagoon Environments, Shimane University, 1060 Nishikawatsu-cho, Matsue, 690-8504, Japan

ARTICLE INFO

Keywords:

The Yellow River delta
Morphological evolution
Critical sediment discharge
Sediment composition

ABSTRACT

The presently active Yellow River (Huanghe) delta lobe has been formed since 1976 when the river was artificially diverted. The process and driving forces of morphological evolution of the present delta lobe still remain unclear. Here we examined the stepwise morphological evolution of the active Yellow River delta lobe including both the subaerial and the subaqueous components, and illustrated the critical roles of riverine discharge and sediment grain size in dominating the deltaic evolution. The critical sediment loads for maintaining the delta stability were also calculated from water discharge and sediment load measured at station Lijin, the last gauging station approximately 100 km upstream from the river mouth. The results indicated that the development of active delta lobe including both subaerial and subaqueous components has experienced four sequential stages. During the first stage (1976–1981) after the channel migration, the unchanneled river flow enhanced deposition within the channel and floodplain between Lijin station and the river mouth. Therefore, the critical sediment supply calculated by the river inputs obtained from station Lijin was the highest. However, the actual sediment load at this stage (0.84 Gt/yr) was more than twice of the critical sediment load (~0.35 Gt/yr) for sustaining the active subaerial area, which favored a rapid seaward progradation of the Yellow River subaerial delta. During the second stage (1981–1996), the engineering-facilitated channelized river flow and the increase in median grain size of suspended sediment delivered to the sea resulted in the critical sediment load for keeping the delta stability decreasing to 0.29 Gt/yr. The active delta lobe still gradually prograded seaward at an accretion rate of 11.9 km²/yr at this stage as the annual sediment load at Lijin station was 0.55 Gt/yr. From 1996 to 2002, the critical sediment load further decreased to 0.15 Gt/yr with the sediment grain size increased to 22.5 μm; however, the delta suffered net erosion because of the insufficient sediment supply (0.11 Gt/yr). In the most recent stage (2002–2013), the intensive scouring of the lower river channel induced by the dam regulation provided relatively coarser sediment, which effectively reduced the critical sediment load to 0.06 Gt/yr, much lower than the corresponding sediment load at Lijin station (~0.16 Gt/yr). Consequently, the subaerial Yellow River delta transitioned to a slight accretion phase. Overall, the evolution of the active Yellow River delta is highly correlated to riverine water and sediment discharge. The sediment supply for keeping the subaerial delta stability is inconstant and varying with the river channel morphology and sediment grain size. We conclude that the human-impacted riverine sediment discharge and grain-size composition play dominant roles in the stepwise morphological evolution of the active delta lobe.

* Corresponding author at: College of Marine Geosciences, Key Laboratory of Submarine Geosciences and Prospecting Technology, Ocean University of China, 238 Songling Road, Qingdao 266100, PR China.

E-mail address: hjwang@mail.ouc.edu.cn (H. Wang).

<http://dx.doi.org/10.1016/j.geomorph.2017.04.042>

Received 23 November 2016; Received in revised form 22 April 2017; Accepted 23 April 2017

Available online 05 May 2017

0169-555X/© 2017 Elsevier B.V. All rights reserved.

1. Introduction

A river delta is a coastal landform resulting from accumulation of substantial quantities of terrestrial sediment near the river mouth, whereby such a deposit can be generally subdivided into subaerial and subaqueous lobes demarcated by the low-tide water elevation limit (Wright, 1977). Deltas nourish half a billion people worldwide and play a critical role in global ecosystem by providing fertile soil and abundant natural resources (Single, 2008; Syvitski, 2008). As the interface between rivers and oceans, deltas are sensitive to global environmental changes. Over the past century, intense human activities in river basins (e.g. damming, irrigation, and soil conservation practices) have sharply decreased the terrestrial sediment delivered to the sea (Milliman, 1997; Syvitski et al., 2005b; Wang et al., 2011), thereby triggering severe erosion of many deltas (Syvitski, 2008), including those of the Nile (El Banna and Frihy, 2009), Colorado (Carrquiry et al., 2001), Mississippi (Blum and Roberts, 2009), Mekong (Le et al., 2007) and Yangtze (Changjiang) (Yang et al., 2003; Yang et al., 2011). Recent studies illustrated that 85% of global river deltas have been subjected to the risk of erosion during the first decade of 21st Century, which has increasingly received more attentions (Syvitski et al., 2009).

The Yellow River (Huanghe), as one of the largest contributors of global riverine sediment to the oceans, had ever delivered 1.08×10^9 t (Gt) of sediment to the sea annually (Milliman and Meade, 1983). Over the past 7000 years, the Yellow River has formed ten delta superlobes along the coasts of the western Bohai Sea and the southern Yellow Sea resulting from its high sediment load and frequent channel migrations (Xue, 1993). The modern Yellow River delta, located in the northeast of Shandong Province (Fig. 1), was formed in 1855 when the Yellow River migrated northward from the Yellow Sea to the Bohai Sea (Pang and Si, 1979). The delta today supports over two million of people and their livelihoods, which includes farming, fishing, and the largest petroleum industry in China (Zhou et al., 2015). In May 1976, the lower Yellow River channel was artificially diverted from the Diaokou course to the Qingshuigou course, and the present-day active Yellow River delta lobe began to develop (Fig. 1B). Given the socio-economic importance and unique ecological environment, the evolution of presently active delta lobe has been the focus of researchers from a variety of disciplines (Yue et al., 2003; Chu et al., 2006; Wang et al., 2009; Cui and Li, 2011; Higgins et al., 2013; Ottinger et al., 2013; Bi et al., 2014).

In addition to the first-order controls to delta evolution including river discharge, sediment supply, tidal and wave regimes, and sea-level rise (Wright, 1977; Orton and Reading, 1993), recent studies (Wang et al., 2006b; Nittrouer and Viparelli, 2014) have shown that river channel morphology and sediment grain size also play critical roles in delta evolution, by modifying the process of delta morphodynamics and altering sediment depositional patterns over the delta at different temporal-spatial scales (Orton and Reading, 1993; Syvitski et al., 2005a). For the Yellow River, the changing regional climate and human activities have had pronounced effects on the delta system, particularly since the 1950s (Wang et al., 2007, 2015). The water and sediment discharge from the Yellow River has experienced stepwise decreases since the 1950s, from $50.15 \text{ km}^3/\text{yr}$ and $1.23 \text{ Gt}/\text{yr}$ during the period of 1950–1968 to $18.19 \text{ km}^3/\text{yr}$ and $0.15 \text{ Gt}/\text{yr}$ during the period of 2000–2005, respectively (Wang et al., 2006a, 2007). Besides the water and sediment discharge, climate change and human activities in the Yellow River basin decreased fine sediment from the Loess Plateau and increased coarse sediment scouring from the lower river channel, and thereby increasing the grain size of suspended sediment delivered to the sea (Wang et al., 2010), which has the potential to modify the physical processes associated with the sedimentary environments and morphological features of the deltaic depositional system (Orton and Reading, 1993). For instance of the Mississippi delta, Kim et al. (2009) indicated that diversion of 45% of the mean annual sand load of the lower Mississippi River would lead to the construction of $\sim 900 \text{ km}^2$ of new land over a century.

Although the importance of river water and sediment to the delta development has been well recognized (Chu et al., 2006; Wang et al., 2006b; Cui and Li, 2011), the impact of the sediment grain size on the evolution of the Yellow River delta still remains unclear. In this study, we examine the evolution of the active Yellow River subaerial and subaqueous delta since the last major river channel shift in 1976. The variations in channel morphology and sediment size, and how these impacted deltaic evolution, are discussed. At a decadal time scale, the deltaic morphology system with a dynamic system (e.g. Yellow River) is dependent not only on the volume of the water and sediment input, but also upon the receiving basin type and the grain size variation. The intense human activities in the Yellow River basin changed the riverine sediment flux and sediment grain size, thereby induced stepwise evolution of the active Yellow River delta. The insights gained from our study will be critical to science community and policy makers to find a sustainable way for balancing the operation of large dams and maintenance of delta system.

2. Study area

As the second largest river in China, the Yellow River originates from the northern Qinghai-Tibetan plateau and then flows eastward through the Loess Plateau and the North China plain, before entering into the shallow semi-closed Bohai Sea (Fig. 1A). Here, the Yellow River builds a typical delta with readily migrating deltaic distributary channels. The system is highly dynamic, whereby in the lower reaches the system have avulsed more than 50 times, thus aiding formation of its delta complex since 1855, when a major channel shift relocated the system to the north side of the Shandong Peninsula (Fig. 1A; Pang and Si, 1979). The active Yellow River delta lobe, located east of the modern Yellow River delta, started to develop in 1976 when the Yellow River was diverted from the Diaokou course to Qingshuigou course in order to facilitate infrastructure construction of the Shengli Oilfield. In 1996, a minor artificial diversion redirected the river channel northward to the Qing 8 (Q8) course for the similar purpose (Fig. 1B). The subaqueous delta we discussed here refers to underwater component of the active Yellow River delta lobe within the 15 m isobath that corresponds to the edge of prodelta (Fig. 1B). Approximately 70%–90% of the terrestrial sediment accumulated close to the river mouth, building a steep subaqueous slope within the 10 m isobath. Nevertheless, a broad delta apron between 12 and 15 m isobaths exists around the entire delta, with an overall regular gradient less than 0.1° (Prior et al., 1986).

The Yellow River delta is a typical river-dominated delta. The tidal regime near the river mouth is dominated by an irregular semi-diurnal tide with a mean range of 0.6–1.3 m. The tidal currents at the river mouth flow southward during flood tide and northward during ebb, with an average speed of 0.5–1.0 m/s (Cheng and Cheng, 2000). The Yellow River delta is in a semi-arid zone subjected to the climate of East Asian Monsoon. A weak southeasterly wind prevails near the river mouth during summer seasons, and a stronger northwesterly to northeasterly wind with a speed more than 10 m/s prevails during winter seasons. The waves off the Yellow River delta are mostly generated by local winds and thus have strong seasonal variability (Zang, 1996). The dominant northerly waves (winter) are much stronger than the prevailing southerly waves (summer). The wind-driven residual current usually moves northward in winter and southward in summer, with a mean velocity of 0.1–0.25 m/s (Pang and Si, 1979).

3. Data and methods

Multi-temporal remote sensing data of Landsat Multispectral Scanner (MSS), Landsat Thematic Mapper (TM) and Landsat Enhanced Thematic Mapper (ETM+) satellite images from 1976 to 2013 were acquired from the Earth Resources Observation and Science (EROS) Center (<http://glovis.usgs.gov/>). Each full MSS, TM or ETM+

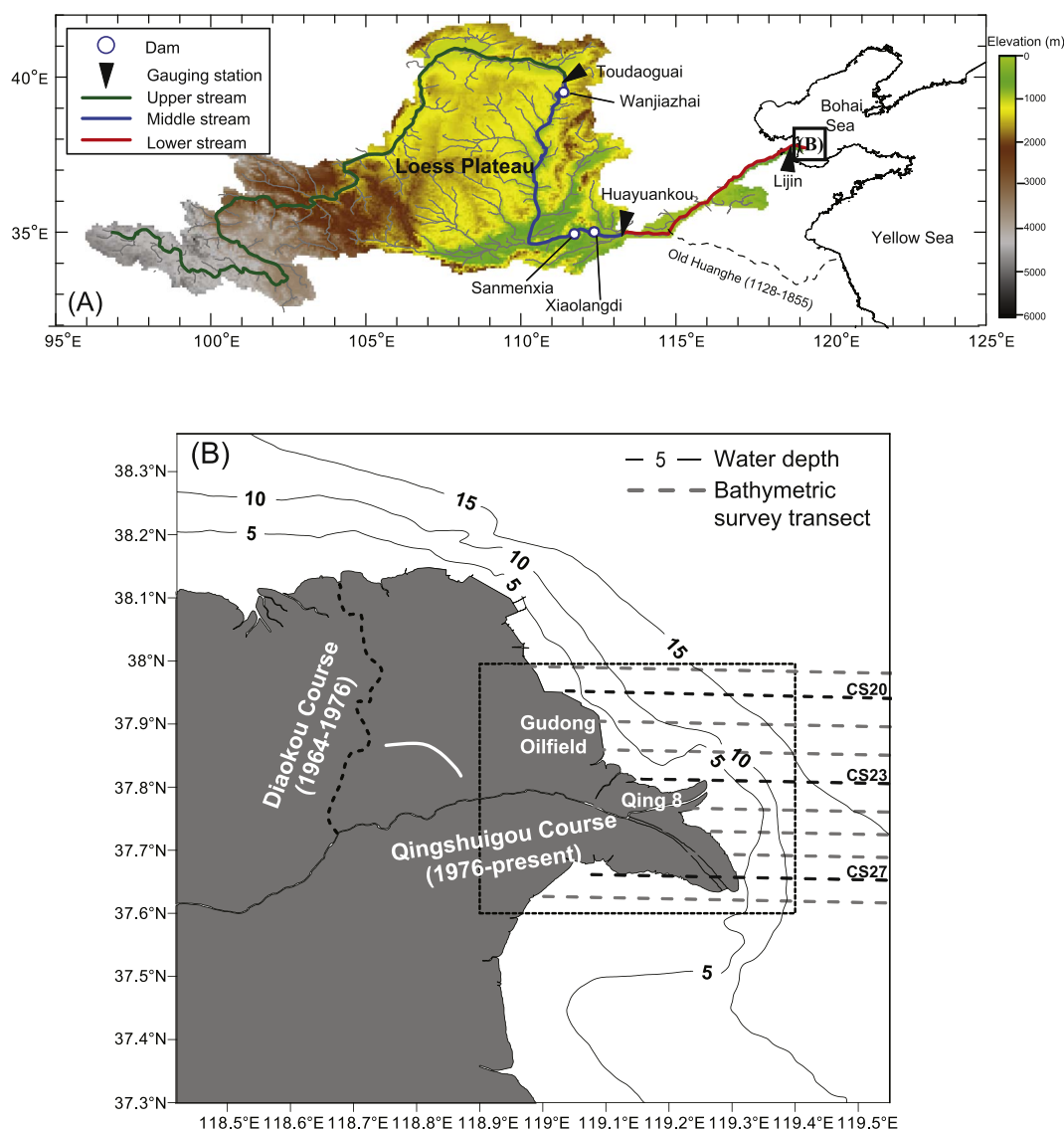


Fig. 1. (A) Map of the Huanghe drainage basin, showing the location of the Lijin gauging stations and reservoirs in the main stream (modified from Wang et al., 2010). (B) Map of the Yellow River delta with the bathymetric transects. The contours of water depth are in meters. The dashed rectangle in panel (B) indicates the location of the active Huanghe delta lobe.

scene can fully cover the study area with the spatial resolution of 60 m, 30 m and 30 m, respectively. The bathymetric data along 10 cross-shore transects right off the active Yellow River mouth (Fig. 1B) from 1976 to 2013, were obtained from the Yellow River Conservancy Committee (YRCC). The bathymetric surveys were conducted annually by using a SDH-13 digital echo-sounder and a UHF-547 microwave positioning device (GPS system for later period). The accuracy of the bathymetry instrument is ± 5 cm for water depth and 2 m for field positioning. The annual water discharge and sediment load, as well as the grain size of suspended sediment, were collected from the Lijin gauging station, ~ 100 km upstream the river mouth (Fig. 1A). In the laboratory at station Lijin, the air-dried suspended sediment samples of every 5 days were analyzed using hand-sieving at 0.25Φ between 1 and 8Φ before 2004 and using Mastersizer 2000 (Malvern Instruments Ltd., UK; the measurement range is $0.02\text{--}2000 \mu\text{m}$) after 2004, and the data were used to calculate the annual grain-size properties (i.e. sorting, skewness, kurtosis and the median grain size).

We extracted a time series of coastline data based on the acquired Landsat imageries. Numerous techniques and methods have been developed for coastline extractions with various applications (Ghorbanali, 2004; Maiti and Bhattacharya, 2009; Higgins et al., 2013). In this study we applied a hybrid method for coastline extraction

as developed by Alesheikh et al. (2007), based on a combination of histogram thresholding and band ratio techniques. Firstly, the histogram of TM band 5 is used for separating land from water. Water pixels are assigned to one and land pixels to zero. Therefore, a binary image named “image No. 1” is achieved. In this case, few land pixels mistakenly have been assigned to water pixels but not vice versa. Secondly, another binary image named “image No. 2” is achieved by the ratio of band 2: band 5. Then the two images are multiplied to obtain a binary image which represents the coastline (Alesheikh et al., 2007). This method separates the water and land directly and accurately, and has been widely used for the Yellow River delta (Cui and Li, 2011; Bi et al., 2014). The delineation of coastline and erosion-accretion patterns of the subaerial and subaqueous delta was achieved using GIS programs MapInfo 7.5, Global Mapper 13.0 and Surfer 11.0. Software SPSS 12.0 was used for the multiple linear regression analysis and correlation analysis in order to calculate the critical sediment load for accretion-erosion balance.

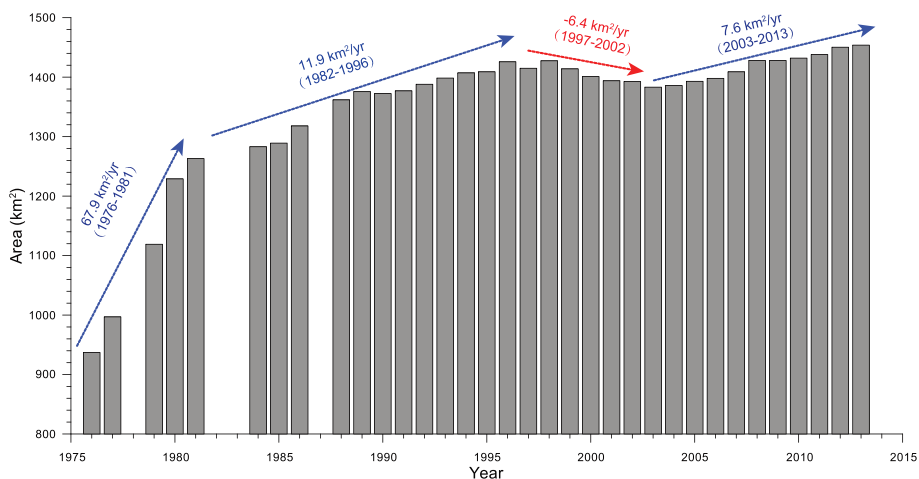


Fig. 2. Variations in the land areas in the active Huanghe delta lobe during the period of 1976–2013, illustrating four stages of delta evolution: a rapid accretion stage (1976–1981), a slow accretion stage (1982–1996), a slow erosion stage (1997–2002), and a slow accretion stage (2003–2013). Land areas in 1977, 1982, 1983 and 1987 are missing due to the cloud cover noise in remote sensing images.

4. Results

4.1. Evolution of the subaerial portion of the active Yellow River delta lobe

The subaerial areas of the active Yellow River delta lobe from 1976 to 2013 were estimated from the extracted shorelines (Fig. 2). The area of subaerial delta increased considerably from approximately 937.0 km² in 1976 to nearly 1453.8 km² in 2013, with an average net accretion rate of 14.0 km²/yr. The general pattern of accretion-erosion of the subaerial delta is divided into four stages (Fig. 2): a rapid accretion stage (1976–1981), a slow accretion stage (1982–1996), a slow erosion stage (1997–2002), and a slow accretion stage (2003–2013). A new delta lobe started to develop rapidly and the coastline began to extensively extend seaward after the shift of the lower river channel in 1976 (Fig. 3). Up to 1981, the land area increased sharply from 937.0 km² (1976) to 1263.0 km², with an average accretion rate of 67.9 km²/yr. Together with the seaward

progradation of delta lobe, the river mouth gradually shifted south-easterly and the width of the protruding lobe tended to become narrower (Fig. 3). Meanwhile, the land area increased more slowly (11.9 km²/yr), from 1263.0 km² in 1982 to 1425.9 km² in 1996 (Fig. 2). In order to control the coastal erosion in Gudong area where a large oil field is located, a coastal dike was constructed in 1984 (Fig. 1B). Since then, the shoreline of the Gudong oilfields has been fixed. In 1996, the lower channel of the Yellow River was diverted to the Q8 course to facilitate the operation of the Shengli Oilfield (Fig. 1B). Due to this artificial diversion of the river channel, a new subdelta lobe began to develop, while the old Qingshuigou subdelta lobe was abandoned and shrunk significantly (Fig. 3). From 1997 to 2002, the total area of the abandoned subaerial delta decreased by 32.0 km², at an average erosion rate of 6.4 km²/yr. From July 2002, the YRCC started to implement the Water-Sediment Regulation Scheme (WSRS) to regulate water and sediment discharges using coordinated operations of three large reservoirs in the middle reaches (Wanjiashai, Sanmenxia

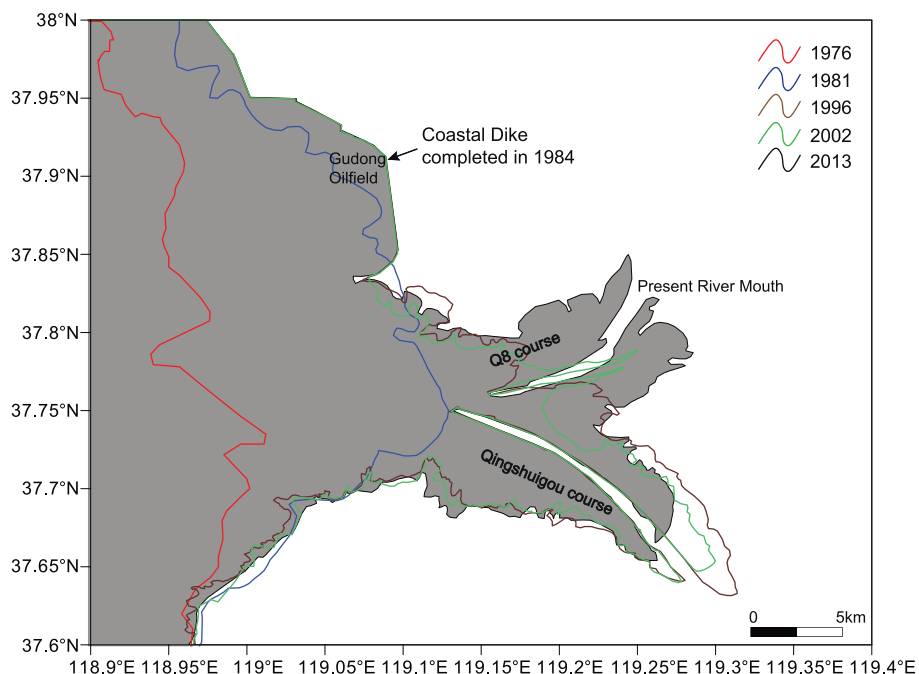


Fig. 3. Part of the shorelines extracted from the remote sensing images in starting year of different stages (1976, 1981, 1996, 2002 and 2013) discerned by variations of land areas in Fig. 2.

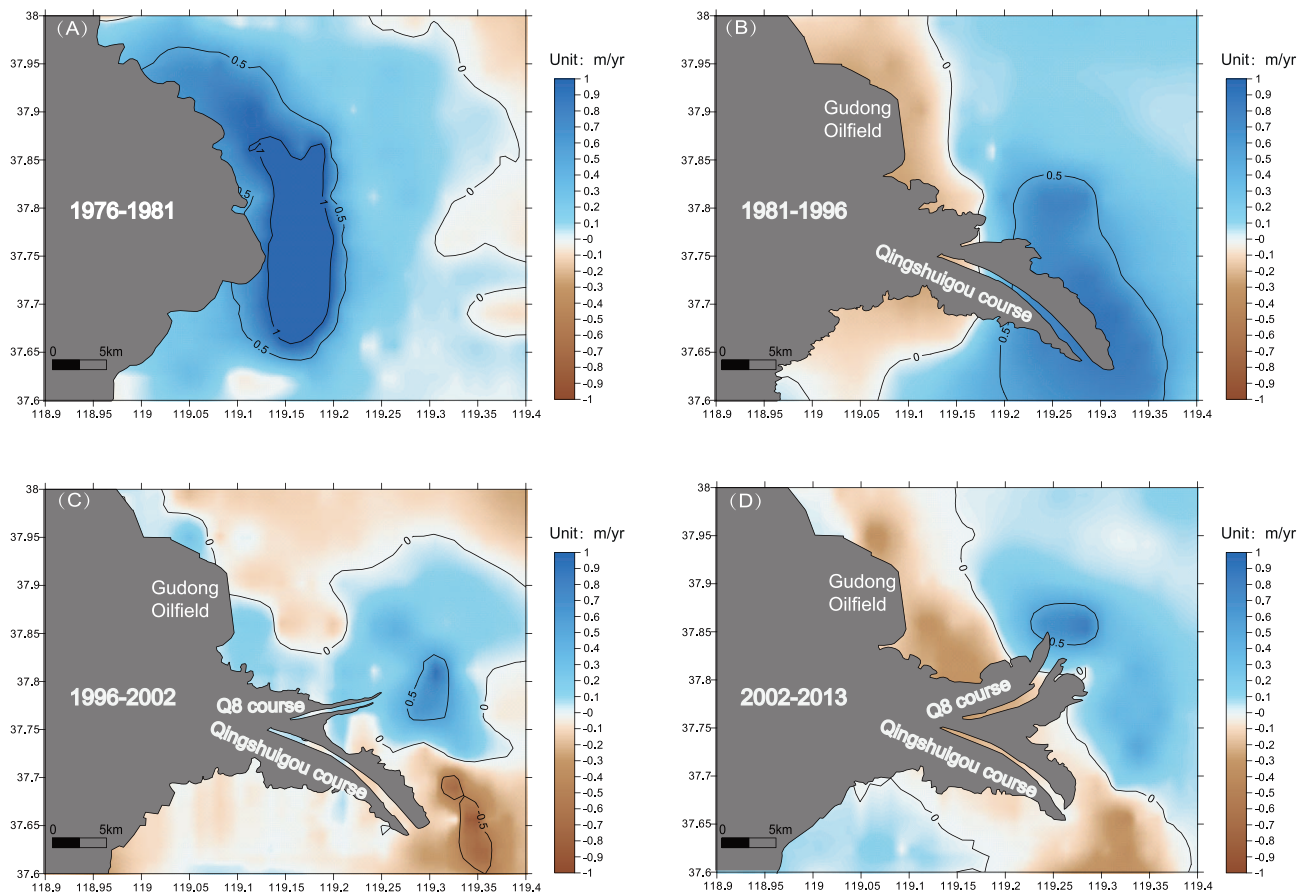


Fig. 4. Spatial variations of accumulation-erosion pattern of the subaqueous Yellow River delta for period of (A) 1976–1981, (B) 1982–1996, (C) 1997–2002 and (D) 2003–2013. The bathymetry survey data were interpolated using Kriging interpolation method. Staged evolution of the subaqueous delta is consistent with that of the deltaic land area.

and Xiaolangdi reservoirs, Fig. 1A). The dam regulation resulted in slow accretion of subaerial delta lobe, with an average progradation rate of $7.6 \text{ km}^2/\text{yr}$ (Fig. 2). During this period, the coastline of Q8 course protruded significantly, and the abandoned Qingshuigou channel retreated continuously (Fig. 3).

4.2. Evolution of the present subaqueous delta lobe

Bathymetric changes of the subaqueous delta between 1976, 1981, 1996, 2002 and 2013, corresponding to the different stages of the subaerial delta lobe, were estimated to examine the temporal and spatial variations of the active subaqueous delta (Fig. 4). During the first stage (1976–1981), accretion was dominant in the entire subaqueous delta with a maximum sedimentation rate of $0.5\text{--}1.0 \text{ m/yr}$ along the coast. The seaward decrease of sedimentation rates suggests that the river sediment predominantly deposited in the shallow area (Fig. 4A). We selected the 5 m and 10 m isobaths of the subaqueous delta as indicators to show the delta progradation. The average progradation rates indicated by 5-m and 10-m isobaths were 464.4 m/yr and 377.2 m/yr , respectively, during the first stage (Figs. 5A, C, Table 1). The progradation of the subaqueous delta from 1976 to 1981 was much slower than that of the subaerial delta during this period, whereby the rate of subaqueous delta growth, as located between the 0–5 m and 5–10 m isobaths, decreased sharply in area by 214.6 km^2 (405 km^2 in 1981 versus 620 km^2 in 1976) and 239.0 km^2 (540 km^2 in 1981 versus 780 km^2 in 1976), respectively (Fig. 5B, D). During the slower accretion stage of the subaerial delta (1982–1996), a depocenter with a mean sedimentation rate of $0.5\text{--}1.0 \text{ m/yr}$ was found near the river mouth, while erosion occurred on both sides of the projecting river mouth (Fig. 4B). In particular, the upper subaqueous delta off of the Gudong

oilfields, where a coastal dike was built in 1984, suffered severe erosion during this period. The 5-m and 10-m isobaths extended seaward with average rates of 407.5 m/yr and 483.8 m/yr , respectively, during the period of 1981–1996 (Table 1). The subaqueous delta area within 5 m and 10 m isobaths increased significantly from 1981 to 1985, and then remained stable with small fluctuations until 1996 (Fig. 5B, D). After the avulsion of the river channel in 1996, the upper subaqueous delta near the river mouth prograded seaward, but the subaqueous delta near the abandoned Qingshuigou course began to retreat due to erosion (Fig. 4C). By 2002, the 5-m isobath had retreated landward with an average rate of -35.4 m/yr , however the 10-m isobath remained stable (Table 1). During this period, the shrinking of the subaerial delta coincided with a slight increase of the area within the 5-m and 10-m isobaths (Fig. 5B, D). Since the implementation of the WSRS in 2002, a depocenter with a maximum sedimentation rate of 0.5 m/yr was found at the nearshore area around the present river mouth, particularly in the upper slope region where water depth is less than 10 m; however, the subaqueous delta near the Gudong oilfields and the abandoned Qingshuigou course has experienced severe erosion (Fig. 4D). During the period of 2002–2013, the 5-m isobath remained stable whereas the progradation rate of the 10-m isobath increased to nearly 114.6 m/yr (Table 1). The accretion of the subaerial delta, in combination with the stable 5-m isobath, resulted in a decrease of the area of the subaqueous delta within 5-m isobath (Fig. 5B).

In addition to these bathymetric changes in terms of accumulation-erosion patterns, the gradient of the subaqueous delta profile has also exhibited substantial changes since 1976 (Fig. 6). A comparison of cross-shore section (CS20) shows a 5 km progradation with an increased slope from 0.93‰ in 1976 to 1.07‰ in 1981, but the steepening trend of the subaqueous delta stopped in 1981 and subse-

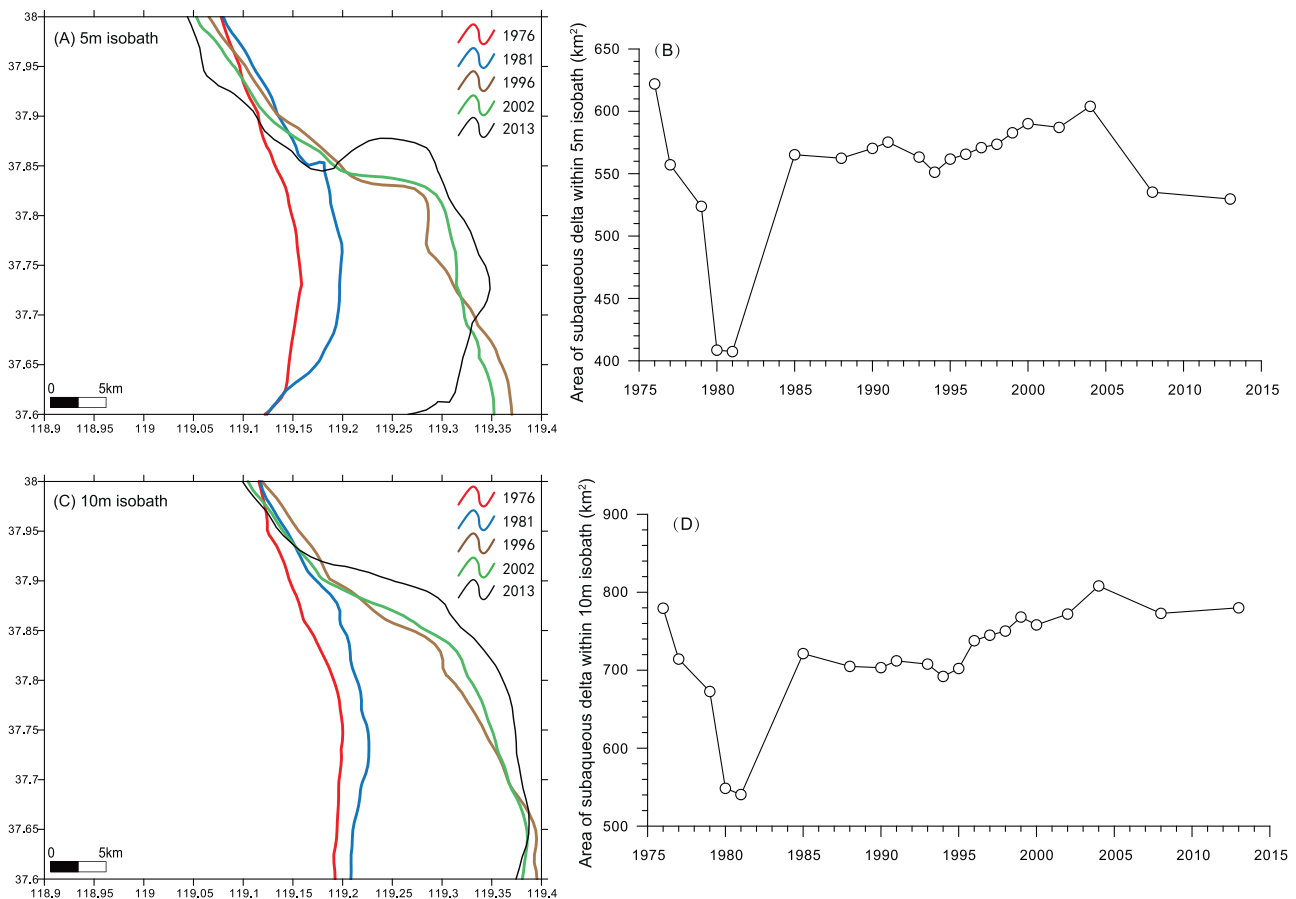


Fig. 5. Shifts of the (A) 5-m and (C) 10-m isobaths in the subaqueous Yellow River delta in starting year of different stages (1976, 1981, 1996, 2002 and 2013). Variation of area within (B) 5 m and (D) 10 m isobaths of the subaqueous delta during the period of 1976–2013. Decrease in the area between the 0–5 m (or 5–10 m) isobaths indicates the progradation/erosion rate of former isobaths is faster/slower than that of latter isobaths, and vice versa.

quently transitioned to be a gentle one (Fig. 6A, Table 2). The subaqueous delta along CS23 profile has prograded continuously since 1976, with a reducing progradation rate after the period of 1981–1996 (Fig. 6B, Table 2). The CS27 was located in the abandoned river mouth (Fig. 1B). The slope along the CS27 remained relatively stable from 0.55‰ in 1976 to 0.56‰ in 1981, but increased significantly to 1.11‰ in 1996 (Fig. 6C, Table 2). Since then, the profile became gentler due to severe erosion of the upper subaqueous delta near the abandoned river mouth (Fig. 4C, D).

5. Discussion

5.1. Relationship between the subaerial deltaic land area and river water and sediment supply

The morphological development of the Yellow River delta is influenced by several key factors, including water and sediment supply, coastal dynamics and morphology of the receiving basin (Chu et al.,

2006; Wang et al., 2006b). The interaction among these factors causes relative ascendancy between progradation and erosion of the delta lobes, thus controlling the growth, shape and slope of the subaerial and subaqueous delta. As the regime of coastal dynamics at the Yellow River mouth has not evidently changed over the past 40 years (Wang et al., 2006b), the alteration of riverine water and sediment supply therefore plays a critical role in the delta evolution. The freshwater flow at the river mouth provides the dynamic condition for sediment transport and deposition, while sediment supply provides the material for land creation in deltas (Coleman and Wright, 1975; Yang et al., 2003). Fig. 7 shows the relationship between delta land area and water supply (Fig. 7A) and sediment supply (Fig. 7B), respectively. As Xu (2002) illustrated, the effects of both water and sediment supply on the evolution of the Yellow River delta need to be evaluated in an integrated way. It is interesting to note that the correlations between land area and river inputs vary significantly over different periods (Fig. 7). Given the relatively constant coastal dynamics at a decadal scale (Wang et al., 2006b), these changes shown in Fig. 7 would be

Table 1
Progradation of 5-m and 10-m isobaths of the subaqueous delta at four stages.

	5 m isobath				10 m isobaths			
	1976–1981	1982–1996	1997–2002	2003–2013	1976–1981	1982–1996	1997–2002	2003–2013
Time interval (yr)	5	15	6	11	5	15	6	11
Progradation distance (m)	2322.1	6112.4	– 212.4 ^a	62.2	1886.0	7256.5	16.9	1260.9
Progradation rate (m/yr)	464.4	407.5	– 35.4 ^a	5.7	377.2	483.8	2.8	114.6

^a Negative values mean erosion.

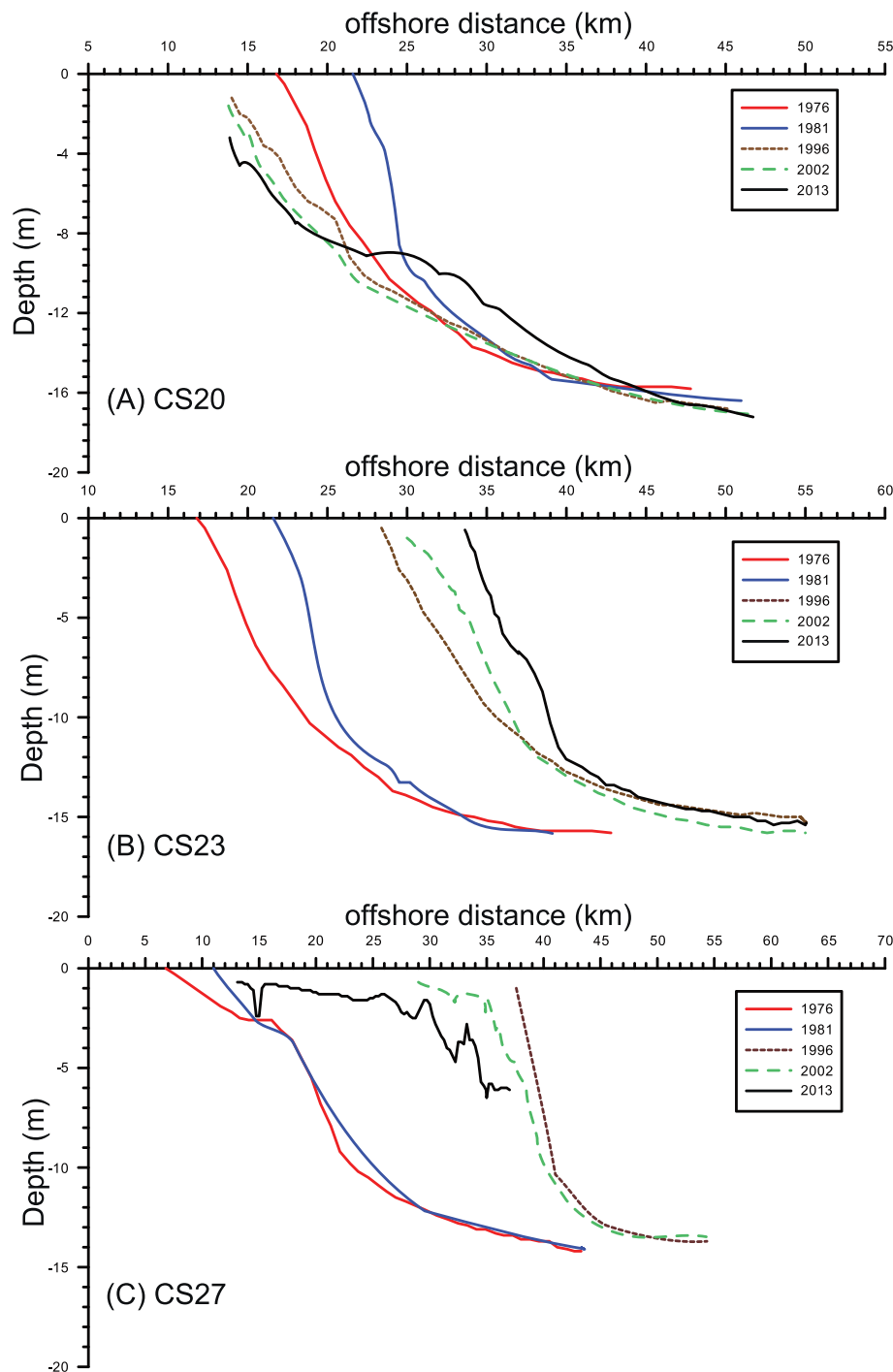


Fig. 6. Bathymetric changes of the subaqueous slope since 1976 at the three cross-shore transects along the active Yellow River delta lobe, to show the evolution of the Yellow River subaqueous delta. Locations of the CS20, 23 and 27 are shown in Fig. 1B.

Table 2
Variation of subaqueous slopes along cross-shore transects of CS20, CS23 and CS27.

Year	slope along CS20 (‰)	slope along CS23 (‰)	slope along CS27 (‰)
1976	0.93	0.94	0.55
1981	1.07	0.98	0.56
1996	0.77	0.96	1.10
2002	0.72	1.02	0.70
2013	0.48	1.07	0.40

induced by the changing river system (e.g. channel morphology, properties of the terrestrial materials and river plume behavior) (Wang et al., 2006b; Edmonds and Slingerland, 2007; Falcini et al., 2012), and should be discussed stage by stage.

Of critical consideration is a threshold value of sediment supply for maintaining the delta stability. In this regard, many previous studies have focused primarily on the correlation between sediment load of the Yellow River and incremental loss or gain of the subaerial delta, while the impact of water discharge has been neglected (e.g. Wang et al., 2006b; Cui and Li, 2011; Kong et al., 2015; Zhou et al., 2015). Moreover, these works did not consider the different characteristics of the staged development of the active Yellow River delta, which makes

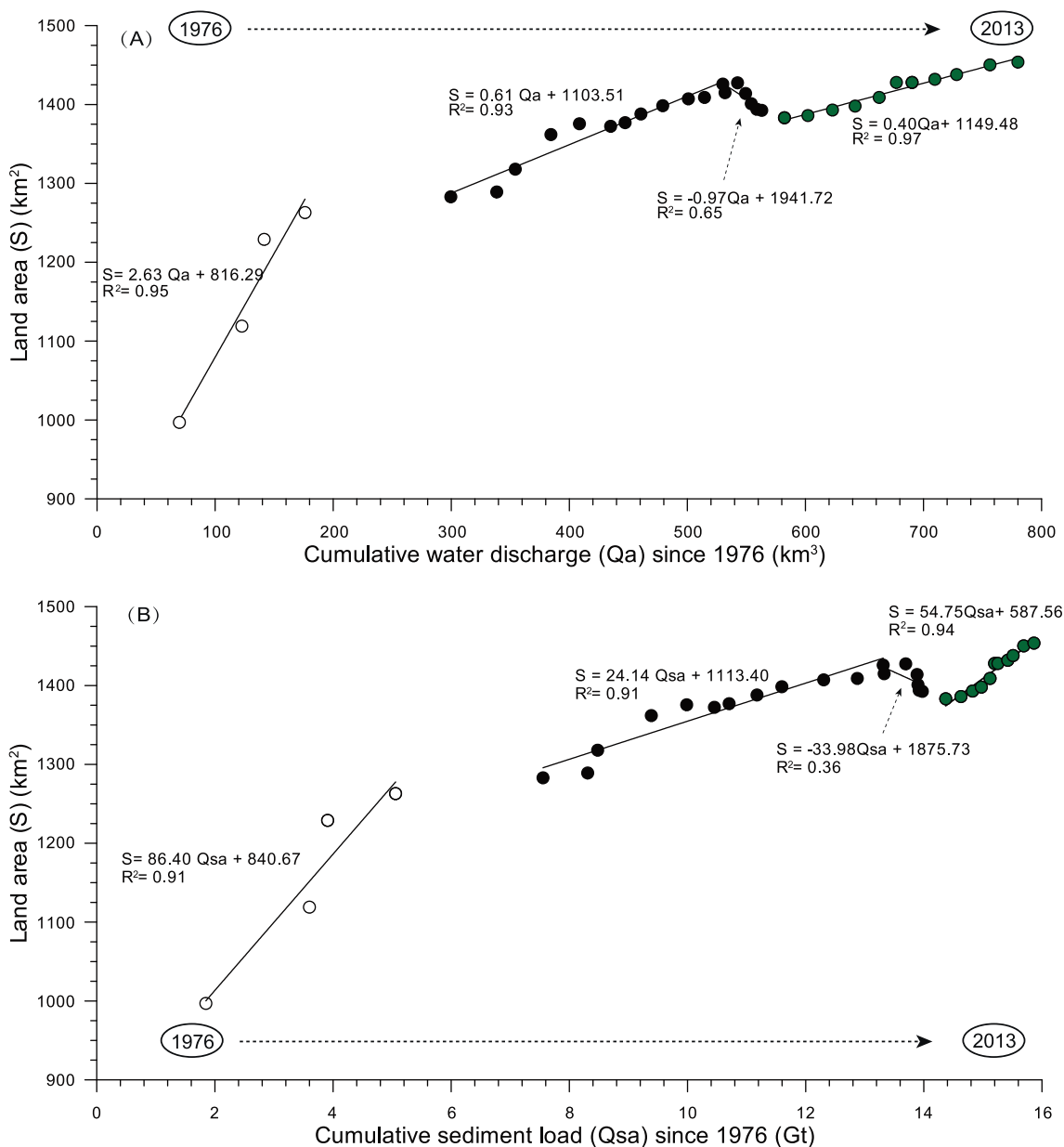


Fig. 7. Relationship between land area of the active Yellow River delta and the cumulative water discharge (A) and cumulative sediment load (B) during the period of 1976–2013. Time progresses from left (1976) to right (2013). The initial values are water discharge and sediment load delivering from the Yellow River to the sea in 1976.

Table 3
Ternary linear regression relationship between land area and river inputs.

	Regression relationship	Correlation between Qa and Qsa	Critical sediment (Gt/yr)
1976–1981	$S = -0.94Qa + 104.54Qsa - 19.72 T + 953.1$ ($R^2 = 0.91$)	$Qsa = 0.02Qa + 0.46$ ($R^2 = 0.88$)	0.35
1982–1996	$S = -0.94Qa + 104.54Qsa - 19.72 T + 953.1$ ($R^2 = 0.91$)	$Qsa = 0.02Qsa$ ($R^2 = 0.99$)	0.29
1997–2002	$S = -2.49Qa + 78.64Qsa - 0.42 T + 1700.5$ ($R^2 = 0.93$)	$Qsa = 0.03Qsa - 4.27$ ($R^2 = 0.80$)	0.15
2003–2013	$S = -2.65Qa + 95.79Qsa - 48.91 T + 954.7$ ($R^2 = 0.99$)	$Qsa = 0.01Qs + 0.05$ ($R^2 = 0.99$)	0.06

Where S is land area; Qa and Qsa are cumulative water discharge and cumulative sediment load from the Huanghe to the sea since 1976, respectively; T is time in years since 1976.

evaluating the delta evolution over various time spans very difficult. Herein, a multi-linear regression analysis is used to account for temporal changes in both water input and sediment supply (Table 3).

Based on the ternary regression model, the cumulative water discharge (Qa) in the equations could be reasonably replaced by the

cumulative sediment load (Qsa) due to their decent correlations (Table 3). If the active Yellow River delta lobe is in equilibrium between accretion and erosion ($\Delta S = 0$), then the annual ($\Delta T = 1$) sediment discharge to the sea (ΔQsa) would become the critical sediment supply for accretion-erosion balance of the Yellow River

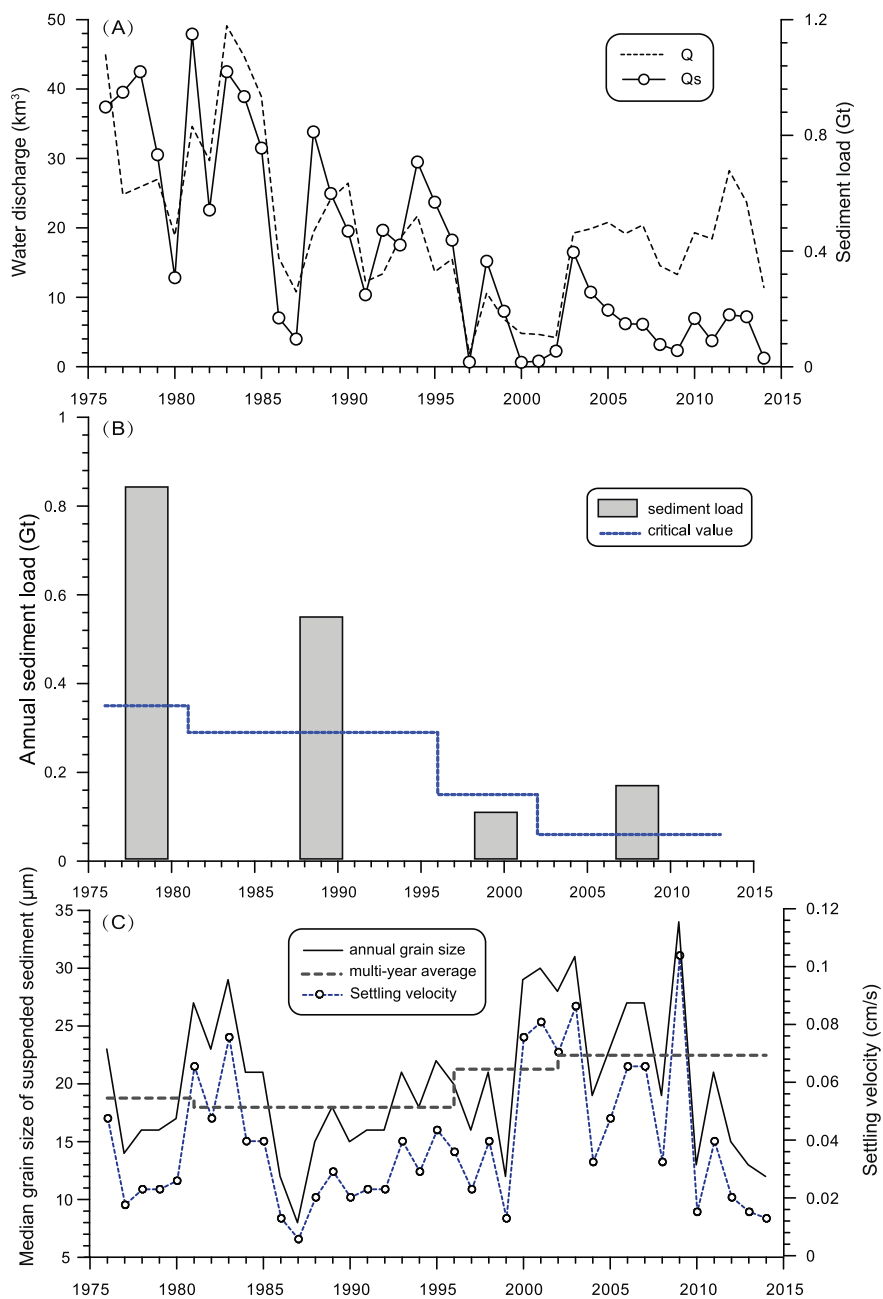


Fig. 8. (A) Time series (1976–2013) of the annual sediment load from the Yellow River to the sea; (B) Actual sediment load and the calculated critical sediment supply in different stages; (C) median grain size and the corresponding settling velocity of suspended sediment reaching the sea from 1976 to 2013. The settling velocity was calculated using the Stokes formula.

delta. The cumulative river inputs we used here were obtained from station Lijin. Inevitably, sediment storage within channels or on the delta surface between station Lijin and the river mouth would influence the calculated critical sediment supply. The results reveal distinct stepwise decreases in critical sediment supply at different stages of the delta evolution (Table 3). From 1976 to 1981, the mean sediment load delivered to the sea was 0.84 Gt/yr (Fig. 8A, B), more than twice of the critical sediment load required for sustaining the subaerial area of the Yellow River delta. Consequently, the delta prograded seaward concomitantly with land area growth (Figs. 2, 3). Along with the decreasing critical sediment load at the second stage of 1982–1996, the sediment delivered from the river to the sea also decreased to 0.55 Gt/yr as a result of climate change and human activities (Fig. 8A, B, Wang et al., 2011). The diminishing discrepancies between actual and critical sediment load make the evolution of the subaerial delta convert to a slow accretion stage during the period of 1982–1996 (Figs. 2, 8B). From

1997 to 2002, the sediment load entering the river mouth further decreased to 0.11 Gt/yr, which is less than the estimated critical sediment load (0.15 Gt/yr) (Fig. 8B). Consequently, the land area of the active delta lobe decreased slightly (Fig. 2). The implementation of WSRS since 2002 has produced artificial flood waters annually as the coarser sediment derived from the lower river bed became a new source of sediment delivered to the delta (Wang et al., 2010). Hence, the average sediment load increased to 0.17 Gt/yr, exceeding the critical sediment load during the period of 2003 to 2013. Therefore, the active delta lobe shifted from a phase of erosion to one of slow accretion after 2003 (Fig. 2).

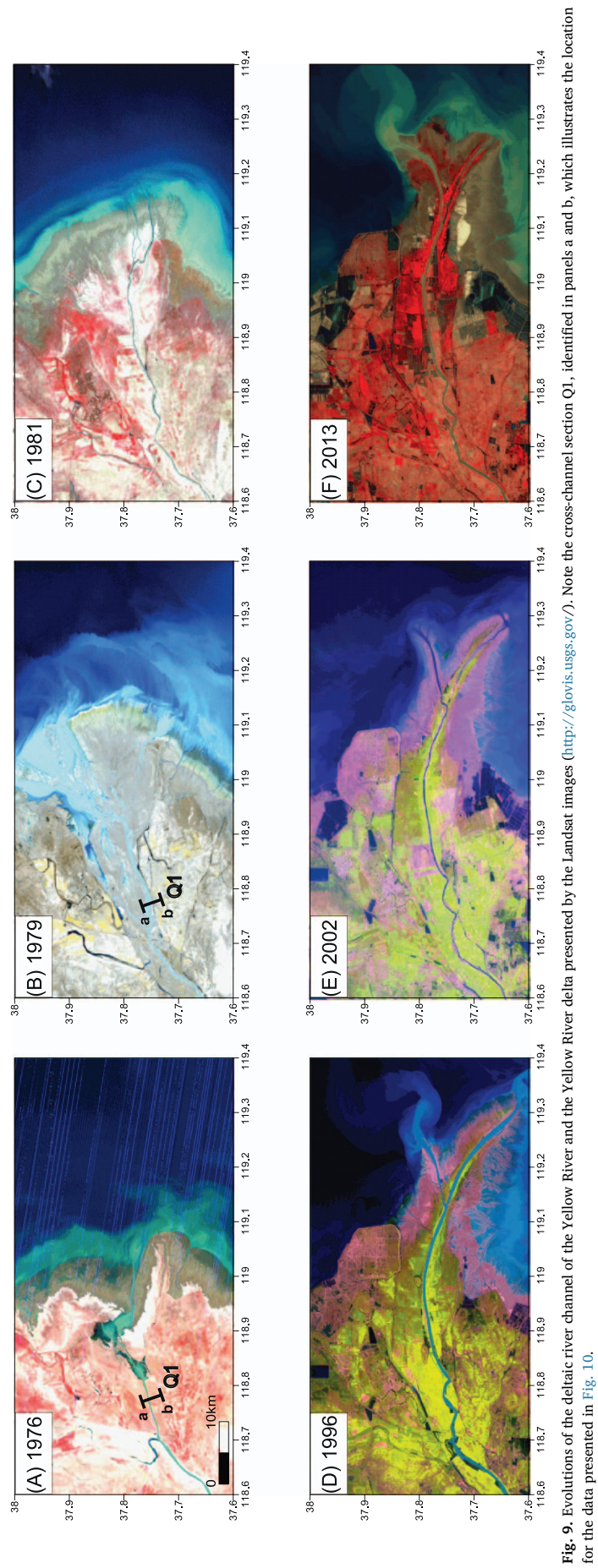


Fig. 9. Evolutions of the deltaic river channel of the Yellow River and the Yellow River delta presented by the Landsat images (<http://glovis.usgs.gov/>). Note the cross-channel section Q1, identified in panels a and b, which illustrates the location for the data presented in Fig. 10.

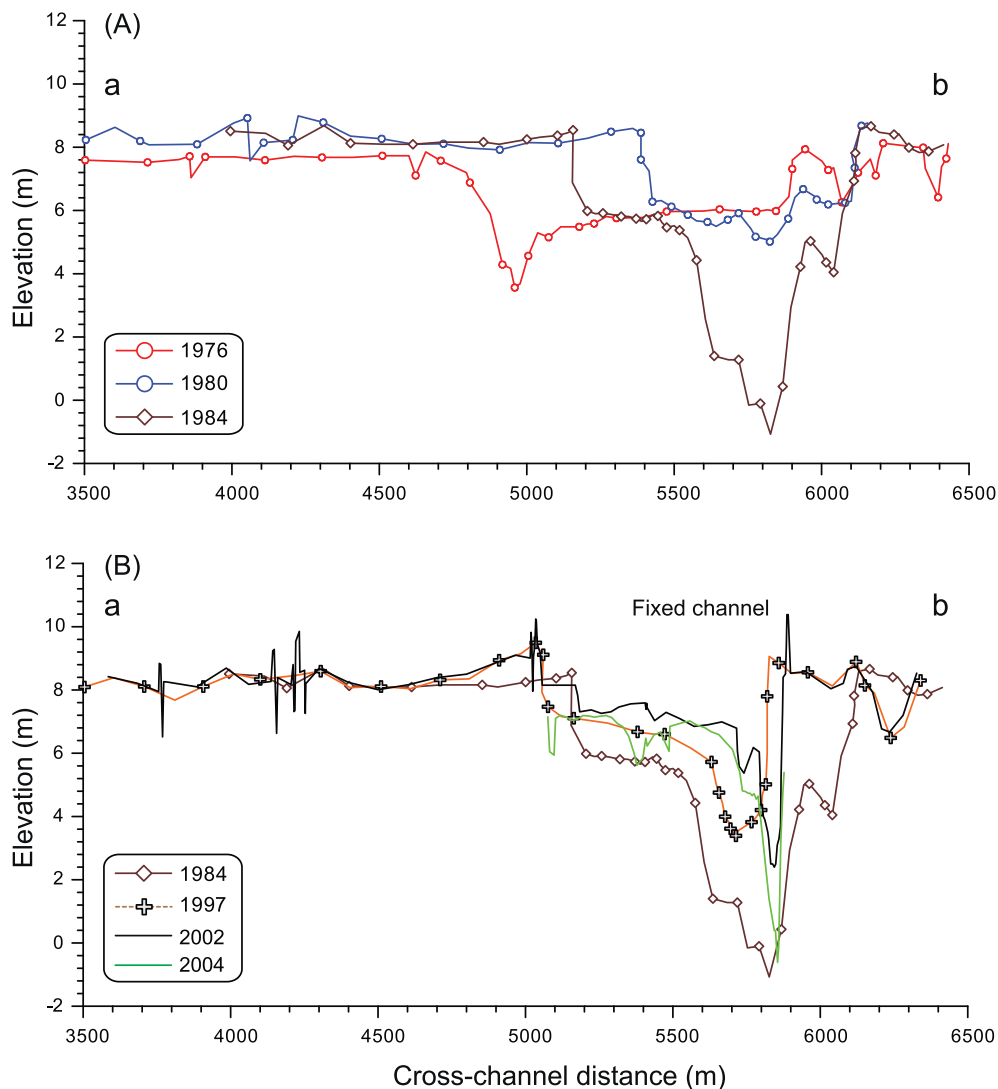


Fig. 10. Variations of channel geometry at cross-channel section Q1 (A: 1976, 1980, 1984; B: 1984, 1997, 2002 and 2004) (modified from Wang et al., 2006b). Section location is shown in Fig. 9.

5.2. Factors controlling the critical sediment load for maintaining the delta stability

5.2.1. Channel morphology

When the lower channel of the Yellow River shifted from the Diaokou course to Qingshuigou course in 1976, the new receiving estuary was a shallow embayment (Fig. 9A). The lower river was initially braided upon relocation, as characterized by unchanneled river flow, until 1981 when the multiple channels coalesced into a single one directed eastward as facilitated by engineering measures (Fig. 9B, C). During this period, the river-derived sediment mostly accumulated on the antecedent subaqueous deltaic plain, filling the shallow embayment area (Wang et al., 2006b). Such a process is clearly illustrated by the changing channel geometry at a cross-channel section, ~ 50.5 km downstream of the station Lijin (line Q1, Fig. 9). Here, significant accumulation occurred among the channels and the floodplain from 1976 to 1980 due to the lack of channelization (Fig. 10A). Lateral migration of the lower channel was active at a rate of ~100 m/yr (Figs. 9, 10A). As a result of vertical aggradation for the channel and floodplain, the actual sediment load contributing to new deltaic land growth was much less than the sediment load recorded at station Lijin. Because the critical sediment load was calculated from the data at Lijin, sediment deficit due to sedimentation among multiple distributary

channels could explain that the critical sediment load for accretion-erosion balance of the subaerial delta during the initial stage (1976–1981) was the highest among the four stages (Table 2). Nevertheless, the subaerial delta still prograded seaward rapidly due to sufficient riverine sediment supply (~0.84 Gt/yr) (Figs. 2, 3, 8B). Moreover, since the Yellow River water discharge was partitioned among multiple channels (Fig. 9A, B), this effectively enlarged the overall hydraulic radius and resulted in lowered flow velocity and sediment transport capacity (Leopold and Wolman, 1960). Thus, much of the total sediment load (including the suspended load) was likely to be captured and accumulated on the delta topset, resulting in rapid expansion of the subaerial delta (Fig. 4A). In contrast, due to the high sedimentation in the subaerial region and the delta topset, the progradation rate of the subaqueous delta at this stage was relatively low, as confirmed by the slight changes of the 5-m and 10-m isobaths (Fig. 5).

Eventually, natural channel adjustments and artificial levee construction resulted in the coalescence of multiple channels into a single channel (Fig. 9C). Under such circumstance, the channelized river flow increased river sediment transport capacity (Leopold and Wolman, 1960). Consequently, the critical sediment supply to maintaining the subaerial delta decreased to 0.29 Gt/yr during the period of 1981–1996 (Table 2) as the sediment bypassing Lijin station could be efficiently

delivered to the river mouth through a single stable channel. Lateral migration of the lower channel stopped at this stage (Fig. 10B). Meanwhile, new land was formed primarily in the vicinity of the seaward protruding river mouth (Fig. 3). As such, during the period of 1982 to 1996, the river mouth extended southeastward due to modification of the river hydrodynamics by tidal and wave currents (Fig. 3). As the river channel prograded away from the adjacent coast (i.e., lobe expansion), southeastward dispersal of river sediment and rapid accumulation around the river mouth ($\sim 0.5\text{--}1.0$ m/yr) produced more steep subaqueous slopes (Table 2; Fig. 6C) that are subjected to slope failures on the delta foreset during extreme conditions such as winter storms (e.g., Prior et al., 1989). The resultant down-slope transport eventually modified the slope to be an equilibrium form. After active channel was abandoned, the subaqueous slope became mild (e.g., CS 27, Fig. 6A) due to erosion-induced sediment reworking.

5.2.2. Sediment grain size

The change of grain size of sediment delivered to the sea substantially impacts the behavior of sediment dispersal and accumulation patterns at the river mouth, particularly as related to resuspension processes due to marine conditions, and thereby modifies the morphology of the subaqueous delta (Orton and Reading, 1993). The coarser sediment particle generally possesses a higher settling velocity and is readily to deposit within the nearshore area off the river mouth (Bi et al., 2014). Moreover, deposition of coarser sediment near the river mouth could modify the texture of seabed to form an armored layer that resists subsequent erosion by wave and tide currents. The average median grain size of the suspended sediment delivered by the Yellow River during the period of 1997–2002 increased to $21.3\ \mu\text{m}$, compared with $18.0\ \mu\text{m}$ during the period of 1982–1996 (Fig. 8C). As a result, the estimated settling velocity of the sediment correspondingly increased to $0.05\ \text{cm/s}$ from $0.03\ \text{cm/s}$, implying a larger contribution to the growth of delta land area. This coincided with the decreasing critical sediment load for maintaining the subaerial delta stability ($\sim 0.15\ \text{Gt/yr}$, see Table 2). Additionally, natural and anthropogenic impacts resulted in the sediment load at station Lijin decreasing to $0.11\ \text{Gt/yr}$ during this period (Fig. 8A; Wang et al., 2007). The active subaerial delta lobe experienced slight erosion from 1982 to 1996 as a result of insufficient sediment supply (Figs. 2, 3). The combined effects of decreasing sediment supply and increasing sediment grain size delivered to the active river mouth resulted in severe erosion on the subaqueous delta. This is especially pronounced near the abandoned Qingshuigou channel lobe, where seabed erodability is high because of rapid deposition in the preceding period (Orton and Reading, 1993). After implementation of the WSRS in 2002, the high river flow scoured the river bed of the lower Yellow River, and the channel erosion became a new and dominant sediment source feeding the delta (Wang et al., 2010). The intensive scouring within the lower reaches provided relatively coarser sediment, increasing the median grain size of suspended particles to $22.5\ \mu\text{m}$ (Fig. 8C) and consequently decreasing the critical sediment load at the last stage (2003–2013) to $0.06\ \text{Gt/yr}$, the lowest among the four stages (Table 3). Because the river-delivered sediment load with large grain size was higher than the critical sediment load during this period (Fig. 8), the subaerial delta transited to a slight accretion phase (Fig. 2). In addition, the WSRS typically operates during summer season when the less energetic coastal environment favors deposition of the coarser sediment, particularly in shallow coastal areas around the river mouth (Wu et al., 2015). Consequently, the depocenter at the nearshore region of the active river mouth continues to develop with a maximum sedimentation rate of $\sim 0.8\ \text{m/yr}$, whereas the subaqueous delta near the Gudong oilfield and around the abandoned river mouth, suffered continuous erosion particularly in the area shallower than $10\ \text{m}$ (Fig. 4D).

At global scale, many river deltas suffer severe erosion due to significant reduction of terrestrial sediment input (Syvitski et al., 2009), and have increasingly received more attentions (Blum and Roberts,

2009; El Banna and Frihy, 2009; Yang et al., 2011). The insights gained from the temporal behavior of the active Yellow River delta lobe indicate that the discharge and grain size of river-laden sediment play a dominant role in delta evolution. The coarse sediment previously accumulated in the lower river channel has become a potential resource for nourishing the delta in a destructive phase (Nittrouer and Viparelli, 2014). The re-delivery of coarser sediment from the lower river channel facilitated by artificial flood during the WSRS of the Yellow River and the rapid response of delta morphology might provide a new insight to maintaining the delta stability and therefore would be a good reference to the management of other large river systems worldwide.

6. Conclusions

Mean high tide lines extracted from Landsat images, in combination with bathymetric data along ten transects off of the active Yellow River mouth, were used to examine the evolution active subaerial and subaqueous Yellow River delta for the period of 1976–2013. The development of the subaerial delta experienced four different stages: rapid accretion (1976–1981), slow accretion (1982–1996), slow erosion (1997–2002), and slow accretion (2003–2013). Correspondingly, the subaqueous delta also experienced different growth/recession patterns at each stage. From 1976 to 1981, rapid sediment accumulation occurred in a large area over the upper subaqueous delta, which effectively steepened the delta slope. From 1982 to 1996, a depocenter was formed near the river mouth, while erosion occurred on both sides of the river mouth. The depocenter shifted to the Q8 channel mouth after an artificial diversion in 1996, and the abandoned Qingshuigou river mouth suffered severe erosion during 1997–2002. After 2002, as impacted by the WSRS, the river-delivered sediment mainly accumulated in the nearshore area, which steepened the subaqueous slope near the present river mouth. Additionally, the slopes on both sides of the river mouth became mild due to significant erosion on the upper slopes.

The evolution of the active Yellow River delta is highly correlated to water discharge and sediment load to the sea. Apart from the volumes of river freshwater and sediment supply, channel morphology and grain size of suspended sediment also influence the short-term evolution of the Yellow River delta. Due to changes in channel morphology and sediment size, the critical sediment load for maintaining the subaerial delta stability has undergone distinct stepwise decreases during 1976–2013. With the reducing sediment load and coarsening sediment size, more sediment deposition took place near the river mouth and caused most of the changes in the erosion-accumulation patterns of the subaqueous delta.

Acknowledgement

We appreciate the constructive comments on the original manuscript from the editor and reviewers. This work was supported by Ministry of Science and Technology of the People's Republic of China (no. 2016YFA0600903), National Science Foundation of China (NSFC, grants no. 41525021, 41476069 and 41376096) and Aoshan talents program supported by Qingdao National Laboratory for Marine Science and Technology (no. 2015ASTP-0503)

References

- Alesheikh, A.A., Ghorbanali, A., Nouri, N., 2007. Coastline change detection using remote sensing. *Int. J. Environ. Sci. Technol.* 4, 61–66.
- Bi, N., Wang, H., Yang, Z., 2014. Recent changes in the erosion–accretion patterns of the active Huanghe (Yellow River) delta lobe caused by human activities. *Cont. Shelf Res.* 90, 70–78.
- Blum, M.D., Roberts, H.H., 2009. Drowning of the Mississippi Delta due to insufficient sediment supply and global sea-level rise. *Nat. Geosci.* 2, 488–491.
- Carriquiry, J.D., Sánchez, A., Camacho-Ibar, V.F., 2001. Sedimentation in the northern gulf of California after cessation of the Colorado River discharge. *Sediment. Geol.* 144, 37–62.
- Cheng, Y.-J., Cheng, J.-G., 2000. Analysis of the current field in the new Yellow River

- entrance sea area. *Coast. Eng.* 19, 5–11 (In Chinese with English abstract).
- Chu, Z.X., Sun, X.G., Zhai, S.K., Xu, K.H., 2006. Changing pattern of accretion/erosion of the modern Yellow River (Huanghe) subaerial delta, China: based on remote sensing images. *Mar. Geol.* 227, 13–30.
- Coleman, J.M., Wright, L., 1975. Modern river deltas: variability of processes and sand bodies. In: *Deltas, Models for Exploration*. Houston Geologic Society, Houston, pp. 99–150.
- Cui, B.-L., Li, X.-Y., 2011. Coastline change of the Yellow River estuary and its response to the sediment and runoff (1976–2005). *Geomorphology* 127, 32–40.
- Edmonds, D.A., Slingerland, R.L., 2007. Mechanics of river mouth bar formation: implications for the morphodynamics of delta distributary networks. *J. Geophys. Res. Earth* 112, F02034.
- El Banna, M.M., Frihy, O.E., 2009. Human-induced changes in the geomorphology of the northeastern coast of the Nile delta, Egypt. *Geomorphology* 107, 72–78.
- Falcini, F., Khan, N.S., Macelloni, L., Horton, B.P., Lutken, C.B., McKee, K.L., Santoleri, R., Colella, S., Li, C., Volpe, G., D'Emidio, M., Salusti, A., Jerolmack, D.J., 2012. Linking the historic 2011 Mississippi River flood to coastal wetland sedimentation. *Nat. Geosci.* 5, 803–807.
- Ghorbanali, A., 2004. Coastline Monitoring by Remote Sensing Technology. MSc thesis 12. Department of GIS Engineeringpp. 18–24.
- Higgins, S., Overreem, I., Tanaka, A., Syvitski, J.P., 2013. Land subsidence at aquaculture facilities in the Yellow River delta, China. *Geophys. Res. Lett.* 40, 3898–3902.
- Kim, W., Mohrig, D., Twilley, R., Paola, C., Parker, G., 2009. Is it feasible to build new land in the Mississippi River Delta? *Eos. Trans. AGU* 90, 373–374.
- Kong, D., Miao, C., Borthwick, A.G.L., Duan, Q., Liu, H., Sun, Q., Ye, A., Di, Z., Gong, W., 2015. Evolution of the Yellow River Delta and its relationship with runoff and sediment load from 1983 to 2011. *J. Hydrol.* 520, 157–167.
- Le, T.V.H., Nguyen, H.N., Wolanski, E., Tran, T.C., Haruyama, S., 2007. The combined impact on the flooding in Vietnam's Mekong River delta of local man-made structures, sea level rise, and dams upstream in the river catchment. *Estuar. Coast. Shelf Sci.* 71, 110–116.
- Leopold, L.B., Wolman, M.G., 1960. River meanders. *Geol. Soc. Am. Bull.* 71, 769–793.
- Maiti, S., Bhattacharya, A.K., 2009. Shoreline change analysis and its application to prediction: a remote sensing and statistics based approach. *Mar. Geol.* 257, 11–23.
- Milliman, J.D., 1997. Blessed dams or damned dams? *Nature* 386, 325–327.
- Milliman, J.D., Meade, R.H., 1983. World-wide delivery of river sediment to the oceans. *J. Geol.* 91, 1–21.
- Nittrouer, J.A., Viparelli, E., 2014. Sand as a stable and sustainable resource for nourishing the Mississippi River delta. *Nat. Geosci.* 7, 350–354.
- Orton, G.J., Reading, H.G., 1993. Variability of deltaic processes in terms of sediment supply, with particular emphasis on grain size. *Sedimentology* 40, 475–512.
- Ottinger, M., Kuenzer, C., Liu, G., Wang, S., Dech, S., 2013. Monitoring land cover dynamics in the Yellow River Delta from 1995 to 2010 based on Landsat 5 TM. *Appl. Geogr.* 44, 53–68.
- Pang, J., Si, S., 1979. The estuary changes of the Huanghe River: 1. Changes in modern time. *Oceanologia ET Limnologia Sinica* 10, 136–141 (In Chinese with English abstract).
- Prior, D.B., Yang, Z.S., Bornhold, B.D., Keller, G.H., Lin, Z.H., Wiseman, W.J., Wright, D.L., Lin, T.C., 1986. The subaqueous delta of the modern Huanghe (Yellow River). *Geo-Mar. Lett.* 6, 67–75.
- Prior, D.B., Suhayda, J.N., Lu, N.Z., Bornhold, B.D., Keller, G.H., Wiseman, W.J., Wright, L.D., Yang, Z.S., 1989. Storm wave reactivation of a submarine landslide. *Nature* 341, 47–50.
- Single, M., 2008. Global change and integrated coastal management: the Asia-Pacific region. *N. Z. Geogr.* 64, 171–172.
- Syvitski, J.P., 2008. Deltas at risk. *Sustain. Sci.* 3, 23–32.
- Syvitski, J.P.M., Kettner, A.J., Correggiari, A., Nelson, B.W., 2005a. Distributary channels and their impact on sediment dispersal. *Mar. Geol.* 222–223, 75–94.
- Syvitski, J.P., Vörösmarty, C.J., Kettner, A.J., Green, P., 2005b. Impact of humans on the flux of terrestrial sediment to the global coastal ocean. *Science* 308, 376–380.
- Syvitski, J.P.M., Kettner, A.J., Overreem, I., Hutton, E.W.H., Hannon, M.T., Brakenridge, G.R., Day, J., Vorosmarty, C., Saito, Y., Giosan, L., Nicholls, R.J., 2009. Sinking deltas due to human activities. *Nat. Geosci.* 2, 681–686.
- Wang, H., Yang, Z., Saito, Y., Liu, J.P., Sun, X., 2006a. Interannual and seasonal variation of the Huanghe (Yellow River) water discharge over the past 50 years: connections to impacts from ENSO events and dams. *Glob. Planet. Chang.* 50, 212–225.
- Wang, S., Hassan, M.A., Xie, X., 2006b. Relationship between suspended sediment load, channel geometry and land area increment in the Yellow River Delta. *Catena* 65, 302–314.
- Wang, H., Yang, Z., Saito, Y., Liu, J.P., Sun, X., Wang, Y., 2007. Stepwise decreases of the Huanghe (Yellow River) sediment load (1950–2005): impacts of climate change and human activities. *Glob. Planet. Chang.* 57, 331–354.
- Wang, L., Yang, Z., Niu, J., Wang, J., 2009. Characterization, ecological risk assessment and source diagnostics of polycyclic aromatic hydrocarbons in water column of the Yellow River Delta, one of the most plenty biodiversity zones in the world. *J. Hazard. Mater.* 169, 460–465.
- Wang, H., Bi, N., Saito, Y., Wang, Y., Sun, X., Zhang, J., Yang, Z., 2010. Recent changes in sediment delivery by the Huanghe (Yellow River) to the sea: causes and environmental implications in its estuary. *J. Hydrol.* 391, 302–313.
- Wang, H., Saito, Y., Zhang, Y., Bi, N., Sun, X., Yang, Z., 2011. Recent changes of sediment flux to the western Pacific Ocean from major rivers in east and Southeast Asia. *Earth Sci. Rev.* 108, 80–100.
- Wang, S., Fu, B., Piao, S., Lü, Y., Ciaisi, P., Feng, X., Wang, Y., 2015. Reduced sediment transport in the Yellow River due to anthropogenic changes. *Nat. Geosci.* 9, 38–42.
- Wright, L.D., 1977. Sediment transport and deposition at river mouths: a synthesis. *GSA Bull.* 88, 857–868.
- Wu, X., Bi, N., Yuan, P., Li, S., Wang, H., 2015. Sediment dispersal and accumulation off the present Huanghe (Yellow River) delta as impacted by the water-sediment regulation scheme. *Cont. Shelf Res.* 111, 126–138 Part B.
- Xu, J.X., 2002. A study of thresholds of runoff and sediment for the land accretion of the Yellow River Delta. *Geogr. Res.* 21 (2), 163–170 (in Chinese with English Abstract).
- Xue, C., 1993. Historical changes in the Yellow River delta, China. *Mar. Geol.* 113, 321–330.
- Yang, S.L., Belkin, I.M., Belkina, A.I., Zhao, Q.Y., Zhu, J., Ding, P.X., 2003. Delta response to decline in sediment supply from the Yangtze River: evidence of the recent four decades and expectations for the next half-century. *Estuar. Coast. Shelf Sci.* 57, 689–699.
- Yang, S.L., Milliman, J.D., Li, P., Xu, K., 2011. 50,000 dams later: erosion of the Yangtze River and its delta. *Glob. Planet. Chang.* 75, 14–20.
- Yue, T.X., Liu, J.Y., Jørgensen, S.E., Ye, Q.H., 2003. Landscape change detection of the newly created wetland in Yellow River Delta. *Ecol. Model.* 164, 21–31.
- Zang, Q.Y., 1996. Nearshore Sediment Along the Yellow River Delta. Ocean press, Beijing (in Chinese).
- Zhou, Y., Huang, H.Q., Nanson, G.C., Huang, C., Liu, G., 2015. Progradation of the Yellow (Huanghe) river delta in response to the implementation of a basin-scale water regulation program. *Geomorphology* 243, 65–74.